Title: On the Origin of Event-Related Potentials Indexing Covert Attentional Selection During Visual Search: Timing Of Selection by Macaque Frontal Eye Field And Event-Related Potentials During Pop-Out Search

Authors: Braden A. Purcell, Jeffrey D. Schall, Geoffrey F. Woodman

Author affiliations:
Department of Psychology
Center for Integrative & Cognitive Neuroscience
Vanderbilt Vision Research Center
Vanderbilt University

Author contributions:
B.A.P., J.D.S., G.F.W. designed research, B.A.P. performed research, B.A.P. analyzed data, B.A.P, J.D.S., and G.F.W. wrote the manuscript.

Running head: Attentional selection by FEF and mN2pc during pop-out.

Keywords: electroencephalogram; covert selection; visual salience; visual attention; top-down control

Corresponding author:
Geoffrey F. Woodman, Ph.D.
Department of Psychology
Vanderbilt University
PMB 407817
2301 Vanderbilt Place
Nashville, TN 37240-7817
geoffrey.f.woodman@vanderbilt.edu
tel: (615) 322-0049

Pages: 44
Figures: 8
Tables: 2

Word count:
Abstract: 243
Introduction: 850
Discussion: 1947

Conflicts of interest: None

Event-related potentials (ERP) have provided crucial data concerning the time course of psychological processes, but the neural mechanisms producing ERP components remain poorly understood. This study continues a program of research in which we investigated the neural basis of attention-related ERP components by simultaneously recording intracranially and extracranially from macaque monkeys. Here, we compare the timing of attentional selection by the macaque homologue of the human N2pc component (m-N2pc) with the timing of selection in the frontal eye field (FEF), an attentional-control structure believed to influence posterior visual areas thought to generate the N2pc. We recorded FEF single-unit spiking and local field potentials (LFP) simultaneously with the m-N2pc in monkeys performing an efficient pop-out search task. We assessed how the timing of attentional selection depends on task demands by direct comparison to a previous study of inefficient search in the same monkeys (i.e., finding a T among Ls). Target selection by FEF spikes, LFPs and the m-N2pc was earlier during efficient, pop-out search than during inefficient search. The timing and magnitude of selection in all three signals varied with set size during inefficient, but not efficient search. During pop-out search, attentional selection was evident in FEF spiking and LFP before the m-N2pc, following the same sequence observed during inefficient search. These observations are consistent with the hypothesis that feedback from FEF modulates neural activity in posterior regions that appear to generate the m-N2pc even when competition for attention among items in a visual scene is minimal.

Event-related potentials (ERPs) provide crucial information on the timing of specific cognitive operations (Luck 2005). Attention-related ERPs can track shifts in attentional allocation in humans processing complex scenes (Woodman and Luck 1999; 2003). Specifically, the N2pc component provides an index of

attentional allocation across the visual field (Luck and Hillyard 1994a; b), but a thorough investigation into the neural mechanisms that generate the N2pc is precluded by the difficulty in obtaining intracranial recordings from human subjects. Current source density and source estimation procedures suggest that the N2pc is generated by attentional modulations in posterior visual regions (Boehler et al. 2011; Hopf et al. 2004; Hopf et al. 2000; Luck and Hillyard 1994a), but these methods are under-constrained without intracranial data (Helmholtz 1853; Luck 2005; Nunez and Srinivasan 2006) and cannot resolve hypotheses concerning the influence of more distal regions that drive the underlying neural generator.

We have addressed this methodological shortcoming by simultaneously recording ERPs with intracranial signals in non-human primates (Woodman 2011). We recently identified a macaque homologue of the N2pc component, termed the m-N2pc, which is a relative positivity contralateral to an attended item (Cohen et al. 2009a; Heitz et al. 2010; Woodman et al. 2007). The human N2pc was originally hypothesized to be due to feedback from attentional-control structures because of its relatively long latency and sensitivity to task-demands (Luck and Hillyard 1994a), but until recently it has been impossible to test this hypothesis directly. ERPs lack the spatial resolution to distinguish the attention-related modulations in visual cortex from control structures in frontal cortex thought to drive those modulations. This has lead to controversy about the degree to which the N2pc reflects bottom-up versus top-down attentional signals (Eimer and Kiss 2010; Theeuwes 2010). Having established a homologous

component in monkeys, we can test this hypothesis using targeted, invasive procedures that are impossible in healthy humans.

The frontal eye field (FEF) is a region of prefrontal cortex thought to be involved in attentional control. FEF single-unit spiking and local field potentials (LFP) evolve to identify the location of behaviorally-relevant search targets (Bichot and Schall 1999; Cohen et al. 2009a; Cohen et al. 2009b; Monosov et al. 2008; Sato et al. 2001; Thompson and Bichot 2005), whether or not a saccade is generated (Thompson et al. 1997; Thompson et al. 2005). For this reason, FEF has been identified with a salience map that guides attentional deployment (Thompson and Bichot 2005), possibly via projections to extrastriate visual cortex (Anderson et al. 2011; Ninomiya et al. 2011; Pouget et al. 2009). The role of FEF in top-down attentional control is further supported by the effects of FEF microstimulation on activity in extrastriate visual cortex (Ekstrom et al. 2008; Moore and Armstrong 2003). Thus, FEF is a prime candidate for an attentional-control structure that could drive the neural generator of the N2pc.

We recently found that FEF neurons and LFPs select the location of search targets before the m-N2pc during an inefficient visual search task (Cohen et al. 2009a). This result is consistent with the hypothesis that feedback from FEF participates in driving the putative posterior generator of the m-N2pc. This hypothesis is also supported by intracranial recordings demonstrating that attentional selection occurs in prefrontal cortex before LIP (Buschman and Miller 2007), V4 (Zhou and Desimone 2010) and IT (Monosov et al. 2010) during attentionally-demanding tasks. However, it is not clear how this timing depends

on task demands. For example, one study has found that the ordering of selection across cortex depends on search difficulty (Buschman and Miller 2007), which could influence the timing of the N2pc relative to FEF. In addition, a recent study reported an N2pc in response to a task-irrelevant singleton (Hickey et al., 2006), suggesting that this component may not depend on top-down influences. Moreover, some theories of visual attention propose that efficient search for a target defined by a single feature can be performed pre-attentively (Treisman and Gelade, 1980). Thus, it could be the case that the onset of the N2pc followed attentional selection in FEF because the task required explicit top-down control, but the same may not hold true during efficient search tasks.

To determine the degree to which the timing of selection in FEF and the m-N2pc depends on attentional demands, we recorded ERPs from monkeys performing an efficient pop-out visual search task simultaneously with FEF single-unit activity and LFPs. The experimental protocol, analytical and statistical methods, and monkeys were the same as those used in a previous report on attentional selection during inefficient T versus L search to allow for direct comparison across studies (Cohen et al. 2009a). If these three signals reflect the timing of attentional allocation, then the timing of selection should modulate with set size when search is inefficient, but not when search is efficient. In addition, if efficient search requires feedback from the saliency map of FEF to the neural generator of the m-N2pc, then we would expect selection in FEF to precede or coincide with the m-N2pc as was observed during inefficient search. We would also expect to see trial-by-trial correlations between FEF activity and the m-N2pc.

MATERIALS AND METHODS

Behavioral tasks and recordings

Recording procedure. We simultaneously recorded neuronal spikes, LFPs, and the extracranial electroencephalogram (EEG) from two male macaques (*Macaca radiata*, identified as Q and S). Monkeys were surgically implanted with a head post, a subconjunctive eye coil, and recording chambers during aseptic surgery under isoflurane anesthesia. Antibiotics and analgesics were administered postoperative. All surgical and experimental procedures were in accordance with the National Institute of Health Guide for the Care and Use of Laboratory Animals and approved by the Vanderbilt Institutional Animal Care and Use Committee.

Neurons and LFPs were recorded from the right and left FEF of both monkeys using tungsten microelectrodes (2-4 MΩ, FHC) and were referenced to a guide tube in contact with the dura. All FEF recordings were acquired from the rostral bank of the arcuate sulcus at sites where saccades were evoked with low-intensity electrical microstimulation (<50 μA; Bruce et al. 1985). Spikes were sampled at 40 kHz and LFPs were sampled at 1 kHz. LFPs were band-pass filtered between 0.2 and 300 Hz and amplified using a Plexon HST/8o50-G1 head-stage. LFPs were baseline corrected using the average voltage during the window from 100 to 0 ms before array presentation. Spikes were sorted online using a time-amplitude window discriminator and offline using principal component analysis and template matching (Plexon Inc.). We generated spike

density functions by convolving each spike train with a kernel resembling a postsynaptic potential (Thompson et al. 1996).

Following the method of Woodman et al. (2007), we recorded ERPs from gold skull electrodes implanted 1 mm into the skull. Electrodes were located at approximately T5/T6 in the human 10-20 system scaled to the macaque skull. EEG signals were sampled at 1 kHz and filtered between 0.7 and 170 Hz. A frontal EEG electrode (approximating human Fz) was used as the reference for the lateral, posterior EEG signals.

Behavioral tasks. The monkeys performed a pop-out visual search task and a memory-guided saccade task, the latter allowed for the classification of different cell types. All tasks began with the monkey fixating a central white spot for ~500ms. In the pop-out visual search task (see Figure 1A), the fixation point changed from a filled to an unfilled white square (10.3 cd/m^2) simultaneously with the presentation of a colored target and one, three, or seven distractors of the opposite color. The number of distractors varied randomly across trials. Targets and distractors were either red (CIE chromaticity coordinates x = 0.620, y = 0.337) or green (CIE x = 0.289, y = 0.605). The target and distractor color remained constant throughout the session and target color was varied across sessions. The monkey was rewarded for making a single saccade to the location of the target within 2000 ms of array presentation and fixating that target for 500 ms.

Each neuron was also recorded during a memory-guided saccade task to distinguish visual- from movement-related activity (Bruce and Goldberg 1985;

Hikosaka and Wurtz 1983). In this task, a target (filled gray disk) was presented for 100 ms at one of eight isoeccentric locations equally spaced around the fixation spot at 10° eccentricity. The animal was required to maintain fixation for 400-800 ms (uniform distribution) after the target presentation. After the fixation point changed from a filled square to an unfilled square, the monkeys were rewarded for making a saccade to the remembered location of the target and maintaining fixation at that remembered location for 500 ms.

We also analyzed previously published FEF neurons, FEF LFPs, and the m-N2pc recorded from the same monkeys during an inefficient visual search (Figure 1B; Cohen et al. 2009a; Cohen et al. 2009b; Woodman et al. 2008). The task was identical to the pop-out search task described above except that monkeys searched for a target defined by form (T or L in one of four orientations) among distractors (Ls or Ts, respectively). Target identity varied across sessions. Analytical and procedural methods were identical for data collected during both tasks. This allowed us to perform statistical comparisons between our new data collected during pop-out search and previously published data collected during inefficient search.

Data analysis

Neuron classification. We identified task-related neurons and LFPs by comparing activity to the baseline period 50 ms before presentation of the array. A neuron or LFP signal was classified as *visually responsive* if activity (discharge rate or voltage) was significantly different from baseline in the interval 50-200 ms

following stimulus presentation during the memory-guided saccade task and in the interval 50-150 ms during search (Wilcoxon rank-sum test, $P < 0.05$). A neuron or LFP was classified as *saccade-related* if activity was significantly different from baseline in the interval -100 to 100 ms relative to saccade initiation for all tasks. Unless otherwise noted, our analyses focused on visually-responsive units with or without saccade-related modulation because these are the neurons known to represent visual salience (Bichot and Schall 1999; Sato et al. 2001; Thompson and Bichot 2005) and likely to project to posterior visual areas thought to generate the N2pc (Gregoriou et al. 2012; Pouget et al. 2009; Thompson et al. 1996). Of the 102 total neurons we recorded, 84 neurons (82%) exhibited significant visual responses. Of the 141 total LFP sites we recorded, 133 LFPs (94%) exhibited significant visual responses. Of the 84 sites in which visually responsive neurons were recorded, 81 (96%) also exhibited visually-responsive LFPs. Thus, the sample size was 81 for the paired comparisons of simultaneously recorded neurons, LFPs, and ERPs. Of the 99 visually-responsive LFP sites in which neurons were concurrently recorded, 18 neurons (18%) did not exhibit visual responses.

Selection time. We used a “neuron-antineuron” approach to determine the selection time when the target location could be reliably discriminated in single-unit spiking, LFPs, and ERPs (Britten et al. 1992; Thompson et al. 1996). The onset of the m-N2pc component is identified as the time when ERPs recorded at posterior lateralized electrodes become different based on the location of the attended target item (i.e., selection time). Here, the selection time is defined as

the time at which the distribution of activity when the search target is inside a receptive field is significantly greater than the distribution of activity when the target is opposite the receptive field for 10 consecutive milliseconds with a conservative α value of 0.01 (Wilcoxon rank-sum test). These criteria are identical to a previous report (Cohen et al. 2009a). For all signals, we defined the receptive field (or preferred location) as the three adjacent target locations in which the firing rate or voltage modulation maximally deviated from baseline. To ensure that our results were not the artifact of the orientation of the corneoretinal potential that changed during the saccade (Godlove et al. 2011b), we also computed selection time with signals aligned on saccade initiation. Only signals which selected the target >20ms before saccade initiation were included in this analysis.

For direct comparison with a previous study, we also estimated selection time by a running an ANOVA at each millisecond following target presentation (Monosov et al. 2008). The resulting p-value gave the probability that the activity did not vary across target locations. The selection time was the first millisecond that the p-value dropped below 0.05 before continuing past 0.001 and remaining below 0.05 for 20 out of 25 subsequent milliseconds. This ensured that differences across studies cannot be explained by differences in analytical methods. This method also ensures that our results are not due to our definition of receptive fields.

We also computed population selection times based on all 102 FEF single-units, 141 LFPs, and the m-N2pc conditionalized on whether the target was

contralateral or ipsilateral to the hemisphere over which the signal was recorded. This approach is more similar to human eletrophysiological studies in which the N2pc is identified by averaging the waveforms from the posterior lateralized electrodes based on whether attention is allocated to the contralateral or ipsilateral visual field. This included neurons and LFP with and without significant visual responses and with both contralateral and ipsilateral preferred locations. Since the average firing rates of cortical neurons vary markedly, we normalized responses between 0 and 1 by subtracting the minimum response and dividing by the range so that variability across recording sites didn't inflate selection times. The population selection time is defined as the time when the distributions of activity when the target is contralateral and ipsilateral significantly diverge for 10 consecutive milliseconds with $\alpha = 0.01$ (Wilcoxon rank-sum test). Here, the distribution is across neurons and recording sites, whereas individual selection times were based on the distribution across trials. All signals were truncated at saccade.

Magnitude of selection. We quantified the magnitude of selection as the difference in response magnitude when the target or a distractor was in the receptive field (preferred location) for each signal. For spiking activity, the magnitude of selection was computed as the difference in average normalized firing rate from 125 to 200 ms after the array presentation. For LFPs and the m-N2pc, the magnitude of selection was computed as the integral of the voltage in the same time window divided by the length of the window (Cohen et al. 2009a). All signals were truncated at saccade.

Set size effects. To assess how RT, selection time, and magnitude of selection depended on set size and search efficiency, we fit a multiple linear regression model of the form,

$$y = \beta_0 + \beta_1 s + \beta_2 e,$$

where the independent variable, *y*, is the mean RT for each session, or the selection time and magnitude of selection for each single-unit, LFP, or ERP. The predictor *s* is the set size (in items) and the predictor *e* is a dummy variable representing search efficiency (0 = efficient, 1 = inefficient). We assessed whether the coefficient β_1 was significantly different from zero to test for significant set size effects. We assessed whether the coefficient, β_2, was significantly different from zero to test for a significant effect of search efficiency.

Visual response latency. The latency of the visual response was determined by comparing baseline activity to activity during a ms-by-ms sliding window starting at array presentation. For FEF spiking activity and LFPs, the visual onset was the time when activity first became significantly different from baseline and remained significant for 10 consecutive ms (Wilcoxon rank-sum test, $p < 0.01$). For ERPs, we required significance to be maintained for 30 consecutive ms to eliminate false alarms indicated by bimodality in the distribution and visual inspection.

Trial-by-trial correlations of spike rate, LFP, and ERP amplitude. We computed the Pearson correlation coefficient between the trial-by-trial amplitude modulation of simultaneously recorded neurons, LFPs, and ERPs. We used only signals that selected the target in these analyses. For spiking activity, amplitude

was computed as the average firing rate in the window from 150 ms after the array presentation until saccadic response to exclude the nonselective initial visual response. For LFPs, amplitude was computed as the integral of the voltage in the same time window divided by the length of the window. We compared simultaneously recorded neurons and LFPs that were recorded from the same electrode or spaced ~1 mm apart. For comparison with a previous study (Cohen et al. 2009a), the ERP amplitude was first computed as the integral of the voltage in the same time window divided by the length of the time window. However, it is possible for this method to yield spurious correlations due to common noise picked up at the frontal reference. As a control, we also computed the ERP amplitude as the integral of the voltage difference between the two posterior electrodes divided by the length of the time window. We computed the correlation using trials in which the target appeared inside the receptive field of the neuron and LFP. As an additional control, we also computed the correlation during the baseline period 100 ms before array presentation. This allowed us to determine the inherent correlations between these signals independent of those elicited by the analysis of the elements in the search arrays. For this analysis, we baseline corrected 250-150 ms before the time window (i.e., 350-250 ms before array presentation).

Control for differences in signal-to-noise ratio. We measured the change in selection time with the number of trials to test whether differences in the signal and noise characteristics of the neural measures could explain observed differences in selection time. Following the methodology of Cohen et al. (2009a),

we characterized the change in selection time as a function of trial number (randomly sampled, with replacement) using an exponential function of the form,

$$ST = ST_{max+min} e^{\frac{-n}{\tau}} + ST_{min},$$

where *ST* is selection time; *n* is the number of trials; τ is the decay (in units of trials); $ST_{max+min}$ is the baseline (ms); and ST_{min} (ms) is the asymptote. We optimized parameters to fit ST as a function of the number of trials individually for each neuron, LFP site, and ERP. If the signal-to-noise ratio is comparable across signals, then the rate of decay, τ, should not vary across signals. If the timing of selection varies across signals, then the asymptote, ST_{min}, should vary across signals despite similar rates of decay.

RESULTS

Behavior

Two monkeys searched for a red or green target stimulus among one, three, or seven distractors of the opposite color (Figure 1A). Both monkeys exhibited behavioral hallmarks of efficient, pop-out visual search. The slopes of RT by set size (i.e., search slopes) were shallow for both monkeys (Figure 1C and Table 1). These search slopes are characteristic of pop-out search in humans (Wolfe 1998) and monkeys (Bichot and Schall 1999). We compared our new efficient search data to previous published data from the same monkeys performing an inefficient search task for a T among L's, and vice versa (Figure 1B; Cohen et al., 2009b). Both monkey's search slopes were significantly shallower during efficient search (Figure 1C; Table 1). During efficient search, the slope of

percent correct by set size was not significant for monkey Q (0.001 ± 0.002; p = 0.43; Wilcoxon rank-sum test) and monkey S (-0.004 ± 0.005; p = 0.72). These results clearly indicate more efficient processing during pop-out search and demonstrate the low attentional demands of the task. It is the neural basis of this difference in processing efficiency which we turn to next.

Selection time

We recorded 102 FEF neurons (48 from monkey S and 54 from monkey Q) that exhibited discharge rate modulations following stimulus presentation or around the time of saccade initiation. This report focuses on the subset of 65/102 neurons (64%) that exhibited spatially tuned visual responses. We also recorded LFP from 141 sites (60 in monkey S and 81 in monkey Q). Of these, 109/141 (77%) exhibited spatially tuned visual responses. The neurons and LFP sites were verified to be in FEF based on low threshold microstimulation (Bruce et al. 1985). During all of these recordings we simultaneously recorded the m-N2pc from EEG electrodes over posterior lateral cortex (Figure 2).

We compared the *selection time,* the time when each signal first reliably signaled the target location, in FEF single-units, FEF LFPs, and the m-N2pc. Figure 2 shows a representative session of simultaneously recorded FEF single-unit spikes, FEF LFPs, and the m-N2pc. All three signals show an initial visual response regardless of the target's location in the visual field. However, each signal evolves over time to discriminate the location of the target stimulus before the saccade is executed. In our example session, the neuron signaled the target

location with an elevated firing rate when the target is inside the RF relative to when it is outside the RF (165 ms after the presentation of the search array; Figure 2A). The LFP recorded from the same electrode, signaled the target location with a greater negativity for the target relative to distractors at approximately the same time (161 ms; Figure 2B). The m-N2pc signaled the target location with a greater positivity contralateral to the target, but this selection did not occur until well after selection by both FEF spikes and LFP (179 ms; Figure 2C).

Figure 3 shows the distribution of selection times for all three signals across our sample of all FEF neurons, FEF LFPs, and concurrently recorded m-N2pc. Overall, the m-N2pc selected the target later (mean ± SE, 192 ± 3.9 ms) than FEF single-unit spikes (160 ± 4.1 ms; $p < 0.001$; Wilcoxon rank-sum test) and FEF LFPs (171 ± 3.9 ms; $p < 0.001$; Table 2). This chronology was also observed when these monkeys performed an inefficient T versus L search task (Cohen et al., 2009a), but average selection time was later in all three signals (single-units: 167 ± 3.6 ms, $p = 0.05$; LFP: 194 ± 3.2, $p < 0.001$; m-N2pc: 202 ± 1.9 ms, $p < 0.001$). In general, the selection time difference between FEF and the m-N2pc was smaller in monkey Q than monkey S (Table 2). One possible explanation is that FEF feedback was integrated and processed more efficiently in the visual cortex of monkey Q, which could explain his superior behavioral performance (mean RT: 223 ± 3.0 ms; percent correct: 97 ± 0.7%) relative to monkey S (mean RT: 254 ± 4.2 ms; percent correct: 83 ± 0.1%), and larger amplitude m-N2pc (4.0 ± 0.47 μV) relative to monkey S (1.9 ± 0.65 μV).

Regardless, it is clear that the m-N2pc never preceded selection in FEF for both monkeys, which is inconsistent with a feed-forward hypothesis. Importantly, selection took place well before mean saccadic response time, indicating that all signals selected the target sufficiently early to have played a role in the covert attention processes that precedes saccade execution. Accordingly, the same pattern of results were observed when we computed selection time with all signals aligned on the time of saccade initiation; the m-N2pc selected the target significantly later (-71 ± 8.7 ms relative to saccade) than both FEF single-units (-113 ± 7.9 ms; $p < 0.01$) and LFP (-105 ± 6.0 ms; $p < 0.01$).

Figures 4A and 4B show that the simultaneously recorded FEF single-units and LFPs typically selected the target before the m-N2pc (Table 2). The average difference between the FEF single-unit selection time and m-N2pc selection time was 23 ± 3.4 ms ($p < 0.001$; Wilcoxon signed-rank test). The average difference between FEF LFP and m-N2pc selection time was 16 ± 2.5 ms ($p < 0.001$). When we recomputed selection time using a running ms-by-ms ANOVA (Monosov et al. 2008), the difference between the m-N2pc and FEF single-units and LFPs remained positive and significant ($p < 0.001$), indicating that this result cannot be due to our selection of preferred locations for each signal. This sequence of selection supports the hypothesis that feedback from FEF contributes to the generation of the m-N2pc even during pop-out search.

One potential explanation is that the m-N2pc is delayed relative to FEF because ERPs are summing across neurons with different RFs. To test for this possibility we also computed population selection times based on all FEF single-

419 units, LFPs, and the m-N2pc conditionalized on whether the target was in the
420 contralateral or ipsilateral hemifield. Analyzed in this way, all three population
421 signals reflect summation across individual signals with different RFs within a
422 hemisphere. Population selection times (±SE, bootstrap, 500 samples) for both
423 FEF single-units (145 ± 18) and LFPs (133 ± 15.8) were still earlier than the m-
424 N2pc (176 ± 27). The population selection time for FEF LFP is earlier than the
425 FEF single-unit selection time because LFP in FEF are more strongly
426 contralaterally biased than single-units (Purcell et al. 2012). It is certain that the
427 contribution of LFPs and single-units to surface ERPs is more complex than
428 simple summation across signals, but this result gives us a degree of confidence
429 that the summation of scattered RFs alone cannot explain our results.

430 We also compared the relative timing of FEF single-units and LFPs to
431 assess mechanisms of efficient target selection within FEF. During inefficient
432 search tasks, FEF single-units select the target before FEF LFPs (Cohen et al.
433 2009a; Monosov et al. 2008). However, across the population of signals, the
434 selection time for FEF single-units and LFPs was not significantly different during
435 efficient search (Figure 3; Table 2; $p = 0.40$; Wilcoxon rank-sum test). Likewise,
436 during efficient search, there was no systematic selection time difference
437 between FEF single-units and LFPs recorded simultaneously on the same
438 electrode (Figure 4C; 0.3 ± 5.1 ms; $p = 0.5$; Wilcoxon signed-rank test). We
439 verified that the selection time difference between FEF single-units and LFP was
440 significantly smaller during efficient search relative to inefficient search task (22 ±
441 3.0 ms; $p < 0.001$). This across-task difference was also evident when selection

time was computed using a running ANOVA method ($p < 0.001$; Monosov et al. 2008). These results show that when search is efficient, the FEF population activity indexed by the LFPs can discriminate the target location as rapidly as individual single-units in the population.

We measured the latency of the initial visual response in each signal to ensure that the differences in selection time were not a consequence of our recording procedures. For example, maybe all electrophysiological activity is earlier when measuring high-frequency spikes or lower frequency LFPs on the microelectrodes relative to the surface ERPs. However, this was not the case. Across monkeys, the mean latency (± SE) of the earliest visual response in each neural signal was 68 ± 2.4 ms for FEF neurons, 56 ± 1.6 ms for FEF LFPs, and 68 ± 2.7 ms for the initial visual ERP component (Table 2). These values are consistent with recent reports (Cohen et al. 2009a; Monosov et al. 2008; Pouget et al. 2005). The visual latency of the FEF LFPs was significantly earlier than both FEF neurons and the posterior ERPs ($p < 0.001$, Wilcoxon rank-sum test), but the mean latency of FEF neurons and posterior ERPs were statistically indistinguishable. The latency of FEF single units is likely similar to the N2pc because the latency of visual responses in FEF is similar to the visual latency of neurons in extrastriate (Schmolesky et al. 1998) and posterior parietal (Andersen et al. 1987) areas thought to contain the electrical fields that directly generate the N2pc. We also computed the selection time during the memory-guided saccade task to ensure that the selection time in the m-N2pc does not consistently trail FEF activity. During the memory-guided saccade task, the mean (±SE) selection

time for the m-N2pc (101 ± 3.1 ms) was not significantly different than the selection time for FEF single-units (105 ± 3.9 ms; $p = 0.94$; Wilcoxon rank-sum test) or LFP (111 ± 4.1 ms; $p = 0.55$), which indicates that selection time differences are specific to the visual search task.

Timing and magnitude of selection during efficient and inefficient search

Previous studies have shown that discrimination of a target from distractors by visually responsive FEF neurons marks the outcome of visual processing for attentional selection (e.g., Thompson et al. 1996, 1997; Sato & Schall 2003). During inefficient search, selection time increases with set size in FEF neurons, LFPs, and the m-N2pc (Bichot et al. 2001b; Cohen et al. 2009a; Cohen et al. 2009b; Sato et al. 2001), which is consistent with delays in the time required to reliably focus attention on the target. Essentially all models of visual attention propose that distractors do not effectively compete for selection during pop-out search (e.g., Duncan and Humphreys 1989; Treisman and Sato 1990; Wolfe 2007). Therefore, if selection time represents an index of attentional allocation, then we would expect it to remain invariant over set size when search is efficient and the target pops out. Indeed, we found that the mean (±SE) slope of selection time by set size during efficient search was not significant for FEF neurons (1.7 ± 1.02 ms/item; $p = 0.09$), FEF LFP (0.6 ± 0.87 μV/item; $p = 0.48$), and the m-N2pc (0.9 ± 0.9 μV/item; $p = 0.32$; linear regression; Figure 5; Table 1). This contrasts sharply with the significant increases in selection time observed during inefficient search for all three signals (FEF single-units: 4.9 ±

1.14 ms/item; $p < 0.001$, FEF LFP: 7.3 ± 0.96 μV/item; $p < 0.001$, m-N2pc: 3.3 ± 0.49 μV/item; $p < 0.001$; Cohen et al., 2009a). The difference in slope of selection time by set size for inefficient search relative to efficient search was significant for all three signals (all $p < 0.001$). This result indicates that selection time increases with the attentional demands of the search task and not simply the number of objects in the visual field.

Previous studies have also found that the amplitude of the N2pc (Luck et al. 1997b; Luck and Hillyard 1994a; 1990) and FEF neurons (Bichot and Schall 1999; Cohen et al. 2009b) depends on attentional demands. During inefficient search, the amplitude of the m-N2pc (Woodman et al. 2007) and FEF neurons (Cohen et al. 2009b) declines with set size. The amplitude of ERP components is related to the variability in the latency (Luck 2005); greater amplitude is expected with lower latency variability and lower amplitude is expected with greater latency variability. Thus, if the latency of the N2pc truly reflects an index of attentional allocation, amplitude should decline with set size during inefficient search when selection time variability increases, but should remain constant with set size during pop-out when selection time variability is constant. We might also expect reductions in the magnitude of the N2pc because the magnitude of discrimination in extrastriate neurons decreases with target salience (e.g., Katsuki and Constantinidis 2012). Indeed, we found that the slope of amplitude by set size during efficient search was not significantly different from 0 for FEF single-units (0.01 ± 0.27 sp/s/item), FEF LFP (-0.01 ± 0.16 μV/item), and m-N2pc (0.04 ± 0.13 μV/item; all $p > 0.05$; Figure 6). In contrast, the average slope of

amplitude by set size during inefficient search significantly declined for FEF single-units (-0.59 ± 0.30 sp/s/item; $p < 0.05$), FEF LFP (-0.35 ± 0.13; $p < 0.001$), and the m-N2pc (-0.19 ± 0.04; $p < 0.001$). This resulted in a significantly smaller magnitude of selection for FEF LFPs and the m-N2pc during inefficient search (LFPs: 3.0 ± 0.56 μV; m-N2pc: 2.2 ± 0.15 μV) relative to efficient search (LFPs: 5.1 ± 0.65 μV, $p < 0.01$; m-N2pc: 3.4 ± 0.47 μV, $p < 0.01$; Wilcoxon rank-sum test). This pattern of modulation is very similar to effects seen in the human N2pc (Eimer 1996; Luck and Hillyard 1990).

We used a bootstrapping procedure to test whether the reductions in m-N2pc amplitude with set size during inefficient search were due to increases in selection time variability. We randomly sampled, with replacement, from all trials recorded during each set size condition, and computed the selection time for the m-N2pc for this subset of trials. The sample size was matched across conditions. This process was repeated 50 times and the standard deviation (SD) of selection time across samples was used as an index of selection-time variability within that condition. Using this procedure, we found that selection time variability was relatively constant during pop-out search (set size 2: SD = 28; set size 4: SD = 27; set size 8: SD = 28), but increased during TL search (set size 2: SD = 25; set size 4: SD = 31; set size 8: SD = 42). This result suggests that increased variability in selection time is at least one contributing factor to reductions in the amplitude of the m-N2pc during inefficient search. Altogether, these results indicate that selection time and amplitude in FEF neurons are

sensitive to attentional demands and extends these observations to LFPs and the m-N2pc.

Trial-by-trial correlation of spike rate, LFP, and ERP amplitude

The similar pattern of modulation in all three signals suggests that FEF may be one source of modulations in posterior visual areas that generate the N2pc. If feedback from FEF is present during pop-out search and influences the neural mechanisms that generate the m-N2pc, then the trial-by-trial amplitude of FEF LFPs should covary with posterior ERP amplitude. The mean correlation between FEF LFP and the m-N2pc was significantly greater than zero (0.53 ± 0.02; $p < 0.001$; Wilcoxon signed-rank test) and comparable to values observed during inefficient search (Cohen et al. 2009a). We verified that the correlation remained significant when performed on the difference in amplitude between posterior surface electrodes (Figure 7A; r = 0.03 ± 0.009; $p < 0.01$), which rules out the possibility that it is simply due to shared noise at the reference. Moreover, this correlation was absent during the baseline period before array presentation ($p = 0.46$) and when only distractors were in the receptive field of the LFP ($p = 0.20$), illustrating both spatial and temporal specificity. It is known that only the superficial layers of FEF feed back to visual cortex (Pouget et al. 2009), which is a likely reason why some LFP sites show negligible correlations with the m-N2pc (Figure 7A). While it is possible that this correlation could be due to either feed-forward or feed-back signals, our observation that selection emerges first in FEF suggests that it reflects feedback. This interpretation is

supported by studies showing a causal effect of microstimulation and pharamacological inactivation of FEF on neuronal activity in posterior visual areas (Ekstrom et al. 2008; Monosov et al. 2011; Moore and Armstrong 2003).

The spike rates of FEF single-units were significantly correlated with LFPs recorded from the same electrode (Figure 7B; r = -0.09 ± 0.008; $P < 0.001$), which is consistent with the hypothesis that LFPs reflect postsynaptic activity of neurons surrounding the electrode tip. This correlation dropped, but remained significant, when it was performed across electrodes spaced ~1mm apart (r = -0.02 ± 0.008; $p < 0.001$), suggesting that these units were nearing the edge of the area over which the LFP integrated (Katzner et al. 2009). In contrast, the mean correlation between FEF spiking and the m-N2pc measured at posterior ERP electrodes was not significantly different from zero (Figure 7C; r = 0.004, $p = 0.61$), which is consistent with studies showing a negligible relationship between these electrophysiological signals (Cohen et al. 2009a).

Control for differences in signal-to-noise ratio across measures of neural activity

A potential concern is that the observed differences in selection time across the electrophysiological signals are due to differences in the signal-to-noise properties of each signal. The pattern of target selection times could just be a difference inherent in the neural measures at different spatial scales. In particular, the signal-to-noise characteristics of the spike times of single neurons may be different from the signal-to-noise characteristics of an LFP derived from a weighted average of ~10^5 neurons within ~1 mm^2 of the electrode tip (Katzner et

al. 2009) and from the signal-to-noise characteristics of an ERP component derived from a weighted average of many cm of cortex (Nunez and Srinivasan 2006) It may be that through summation, the LFPs and ERPs become more reliable measures, or the summation may introduce more noise into the LFP and ERP. Following Cohen et al. (2009a), we reasoned that the signal-to-noise characteristics of each neural signal will determine how increasing trial numbers affects the reliability with which the target can be discriminated (see also Bichot et al. 2001b). We fit an exponential curve to selection times as a function of trial number measured from FEF neurons, LFP, and the m-N2pc. The average number of trials per session was greater than the number of trials necessary for all signals to reach asymptote (Figure 8A, black point). The rate of decay, *τ,* was statistically indistinguishable for neurons (101 ± 26.4; median ± SE), LFP (139 ± 33.0), and the m-N2pc (129 ± 24.9; Figure 8B; all $p > 0.09$; Wilcoxon rank-sum test). In a previous study of inefficient search (Cohen et al. 2009a), the corresponding values were 94 ± 14.2, 144 ± 21.7, and 97 ± 17.5 for neurons, LFP, and the m-N2pc, respectively (all $p > 0.14$). This result is consistent with the comparable confidence intervals that are apparent in Figure 2. However, the level at which selection time reached asymptote was lowest for neurons (138 ± 4.3), followed by LFP (150 ± 4.2), and latest by the m-N2pc (180 ± 4.0; Figure 8C; all $p < 0.05$, Wilcoxon rank-sum test). This result is consistent with the ordering of selection times reported above (Figure 3). In a previous study of inefficient search (Cohen et al. 2009a), the corresponding values were 151 ± 3.2, 172 ± 5.2, and 188 ± 2.7 for neurons, LFP, and the m-N2pc, respectively (all $p <$

602 0.01). Thus, we can conclude that the timing differences across the signals are
603 not due to different signal-to-noise characteristics of the neural measures.
604
605 **DISCUSSION**
606 To understand the neural mechanisms that generate attention-related
607 ERPs, we recorded the macaque homologue of the N2pc component
608 simultaneously with single-unit spiking and LFPs in FEF. We asked how the
609 timing of selection in all three signals depends on the attentional demands of the
610 task by directly comparing the timing of selection during an efficient pop-out
611 search task with an inefficient form search task (Cohen et al. 2009a). We
612 showed that both the timing and magnitude of selection in all three signals
613 depends on the attentional demands of the task. However, selection was evident
614 in FEF before the m-N2pc regardless of search efficiency. These results are
615 consistent with the hypothesis that the primate N2pc is due to feedback from
616 higher cortical areas, even when bottom-up salience is sufficient for task
617 performance. These results also inform us about the neural mechanisms that
618 generate the N2pc and constrain theories of visual attention.
619
620 *Comparison of human and macaque N2pc*
621 Before we consider the relevance of our findings to the study of human
622 ERPs, we must first ask whether the macaque m-N2pc indexes the same
623 cognitive operations as the human N2pc. The m-N2pc satisfies several
624 established criteria for across-species homology (Woodman 2011). Previous

studies have shown that the spatial distribution of the N2pc is maximal over posterior electrodes in both humans (Luck and Hillyard 1994a) and monkeys (Cohen et al. 2009a; Woodman et al. 2007). In addition, previous studies have found that the latency of the N2pc increases with set size in both humans (Luck and Hillyard 1990) and monkeys (Woodman et al. 2007) when search is inefficient. We found that the latency and amplitude of the macaque N2pc (m-N2pc) are insensitive to changes in set size during efficient pop-out search, which is consistent with an index of attentional demands and not simply the number of objects on the screen. We also found that the amplitude of the m-N2pc is greatest during efficient search, which is observed with the human N2pc (Eimer 1996). Thus, the m-N2pc satisfies multiple criteria for homology including a similar spatial distribution, task dependence, and timing. Our findings provide new support for this across-species homology.

One notable across-species difference is that the polarity of the N2pc is reversed. Humans show a contralateral negativity and monkeys show a contralateral positivity. This is likely due to differences in cortical folding in posterior visual areas across the species. For example, macaque V4 is located on the surface of the prelunate gyrus (Zeki 1971), but the human homologue spans several sulci (Orban et al. 2004). Another potential across-species difference is that several studies of the human N2pc have reported increases in amplitude with attentional demands (Hopf et al. 2002; Luck et al. 1997b), whereas we observed declines in the m-N2pc. This is likely due to differences in task design rather than species. In humans, this effect is observed when targets

and distractors are tightly grouped in a limited portion of the visual field. In contrast, when stimuli are well spaced across hemifields as in our monkey studies, amplitude decreases with additional stimuli (Eimer 1996). Future experiments that compare the N2pc observed in humans and monkeys under identical experimental design (e.g., Godlove et al. 2011a; Reinhart et al. 2012a; Reinhart et al. 2012b) can further establish the homology across species.

The origin and interpretation of the N2pc

We found that the pattern of modulation in FEF LFP and the N2pc were similar during inefficient and efficient visual search and the signals were correlated on a trial-by-trial basis. This suggests that FEF is influencing the generation of the N2pc, but it seems unlikely that the contribution is direct. First, voltage distributions, current source density topography, and dipole source modeling suggests that the dipole seen as the N2pc on the scalp originates in posterior visual cortex in humans (Hopf et al. 2004; Hopf et al. 2000; Luck et al. 1997a) and monkeys (Cohen et al. 2009a; Woodman et al. 2007; Young et al. 2011). Second, the timing differences that we observed seem inconsistent with identification of FEF as the direct neural generator because extracranial EEG is not delayed relative to intracranial synaptic activity (Givre et al. 1994; Nunez and Srinivasan 2006). However, both the human and the macaque N2pc is not observed at anterior electrodes near FEF (Woodman et al. 2007; Cohen et al. 2009). How can this be? Two possibilities are consistent with what we assume occurring in the working brain. First, the electrical fields generated in FEF might

be actively canceled by electric fields of the opposite polarity in nearby cortical areas. Second, it is possible that the dipole is simply oriented parallel to the skull such that it does not produce an observable extracranial signal. Future recordings from multiple intracranial electrodes will provide more detailed information about the configuration of the electrical fields in prefrontal cortex and distinguish between these explanations.

Instead, these observations are consistent with the hypothesis that FEF is part of a frontal-parietal network involved in driving attentional shifts in posterior visual areas thought to generate the m-N2pc (Corbetta 1998). FEF is part of a distributed network of structures shown to encode a representation of visual salience for guiding attentional deployments (Thompson and Bichot 2005). Our observation that activity in FEF modulates concurrently with the m-N2pc during both efficient and inefficient search suggests that this network is engaged regardless of search efficiency. Some studies have questioned the need for an influence of frontal structures during efficient search tasks based on BOLD responses (Leonards et al. 2000) and effects of transcranial magnetic stimulation (Muggleton et al. 2003) in prefrontal areas during inefficient, but not efficient search. However, these results are inconsistent with findings from monkey studies showing that reversible inactivation of FEF with the GABA agonist muscimol impairs performance on pop-out search tasks (Monosov and Thompson 2009; Wardak et al. 2006). In addition, other studies report comparable BOLD activation in human (Anderson et al. 2007) and monkey (Wardak et al. 2010) FEF irrespective of search efficiency. Thus, our results add

694 to converging evidence suggesting that FEF plays an important role in
695 processing visual targets even during efficient search tasks.

696 Our results also inform the interpretation of the cognitive processes indexed
697 by the primate N2pc. The degree to which the human N2pc reflects the initial
698 spatial selection of a target or post-selection processing has been unclear (Eimer
699 and Kiss 2010; Theeuwes 2010). Our data place clear limits on the degree to
700 which the latency of the N2pc can be interpreted as the time of initial spatial
701 selection because the N2pc followed selection in prefrontal cortex even during an
702 efficient search task that required minimal feature analysis. One limitation of the
703 current task design is that the singleton was always task relevant, and therefore
704 we cannot make strong claims about the relative timing of selectivity based on
705 pure bottom-up physical salience. However, our results are consistent with a
706 growing body of work demonstrating the sensitivity of the N2pc to top-down
707 factors and extend that work by suggesting that FEF is a likely source of this top-
708 down modulation. When a color singleton is not task relevant, the N2pc is small
709 or absent (Eimer et al. 2009; Luck and Hillyard 1994a) and selectivity in FEF is
710 minimal (Bichot et al. 2001a). The N2pc is also sensitive to rewards associated
711 with target localization and identification (Kiss et al. 2009), as are FEF neurons
712 (Ding and Hikosaka 2006). Lastly, trial history and experience influence both the
713 N2pc (An et al. 2012; Eimer et al. 2010) and FEF neurons (Bichot and Schall
714 1999; 2002; Bichot et al. 1996). The same FEF neurons that are modulated by
715 these top-down factors project to earlier visual areas thought to generate the

716 N2pc (Pouget et al. 2009), which is consistent with the hypothesis that FEF is the
717 source of these modulations.
718
719 *Relation to previous studies of attentional selection across cortex*
720 Several recent studies have investigated the timing of attentional selection
721 across cortex using paired intracranial recordings. Zhou and Desimone (2011)
722 observed earlier selection in FEF neurons relative to V4 neurons during an
723 inefficient conjunction search tasks. Similarly, during inefficient conjunction
724 search, Buschman & Miller (2007) observed earlier selection in FEF and
725 dorsolateral prefrontal neurons. In addition, Monosov et al., (2010) found that
726 FEF neurons exhibited significant spatial selectivity before IT neurons exhibited
727 significant object selectivity during a difficult search and identification task. Thus,
728 converging evidence supports the hypothesis that attentional selection in FEF
729 neurons precedes attentional selection in several earlier visual areas when tasks
730 are attentionally demanding (see also Cohen et al. 2009a), but findings during
731 efficient pop-out search are less consistent. One study found that selectivity in
732 lateral intraparietal area precedes selectivity in FEF and dorsolateral prefrontal
733 cortex during pop-out search (Buschman and Miller 2007), but a recent study
734 found the opposite; frontal areas selected before parietal areas during pop-out
735 (Katsuki and Constantinidis 2012). In addition, studies using nearly identical task
736 designs and analytical methods found that both FEF and LIP select the location
737 of a color singleton at approximately the same time (Thomas and Pare 2007;
738 Thompson et al. 1996). Our observation that the m-N2pc selects the target

location later than FEF is consistent with studies suggesting that FEF selectivity precedes selectivity in early visual areas, but it is important to note that ERPs cannot be regarded as a direct proxy for underlying neural activity. ERPs are thought to reflect the summation of synchronous activity across many centimeters of cortex (Nunez and Srinivasan 2006), and the N2pc likely reflects attentional selection across multiple visual areas. Thus, additional simultaneous recordings in frontal and parietal areas will be necessary to conclusively determine the degree to which the timing of selection across neurons in different cortical areas depends on task demands.

In addition to our observations regarding the timing relationship between FEF and the m-N2pc, we also observed differences in the relative timing of selection in FEF single-units and LFP depending on the attentional demands of the task. Previous studies have found that FEF LFPs select the target later than FEF single-units (Cohen et al. 2009a; Monosov et al. 2008). We found that the delay in selection time between FEF single-units and LFPs was absent during pop-out. LFPs reflect the synaptic activity of thousands of neurons surrounding the electrode tip (Katzner et al. 2009; Mitzdorf 1985), whereas spiking activity reflects only a single neuron. Therefore, one interpretation of this result is that the population of FEF neurons contributing to the LFP reached a consensus about target identity more efficiently during pop out. The absence of a delay between selection in FEF single-units and LFP was unexpected given a previous report showing a significant delay between the two signals in one monkey performing a covert pop-out search task in which target location was reported via

762 lever turn (Monosov et al. 2008). Covert visual search requires active
763 suppression of saccade generating neurons in FEF (Thompson et al. 2005),
764 which could have postponed LFP selectivity. In line with the present findings,
765 another interpretation is that the delayed LFP selection time relative to single-
766 units during covert search reflects the increased attentional demands required to
767 map target location to the lever turn.
768
769 *Relation to theories of visual search and attention*
770 Early models of visual attention proposed that targets that could be
771 distinguished by a single feature could be localized “pre-attentively” solely
772 through bottom-up selection of local feature differences (Itti and Koch 2001;
773 Treisman and Gelade 1980). Other studies have shown that prior knowledge
774 and expectation have a strong influence on pop-out performance (Joseph et al.
775 1997; Maljkovic and Nakayama 1994; Treisman and Gormican 1988). Our
776 finding that an attentional control area, FEF, contributes to the generation of the
777 N2pc during efficient search is consistent with theories of visual attention that
778 propose no strong dichotomy between efficient and inefficient search (Bundesen
779 et al. 2005; Desimone and Duncan 1995; Treisman and Sato 1990; Wolfe 2007).
780 This result is consistent with a recent study which found that the enhanced
781 response of V4 neurons to a pop-out stimulus is eliminated when attention is
782 directed elsewhere in the visual field (Burrows and Moore 2009). Thus, our
783 findings add to behavioral and neurophysiological evidence that top-down input
784 from frontal cortex may guide attentional selection even during pop-out search.

Acknowledgements: This work was supported by National Institutes of Health Grants T32‐EY07135, R01-EY019882, R01‐EY08890, P30‐EY008126, P30‐HD015052, and Robin and Richard Patton through the E. Bronson Ingram Chair in Neuroscience. We thank J. Cohen and R. Heitz for collecting the inefficient search data. Requests for materials should be addressed to G.F.W. (e-mail: geoffrey.f.woodman@vanderbilt.edu) or J.D.S. (e-mail: jeffrey.d.schall@vanderbilt.edu).

REFERENCES

An A, Sun M, Wang Y, Wang F, Ding Y, and Song Y. The N2pc Is Increased by Perceptual Learning but Is Unnecessary for the Transfer of Learning. *PLoS One* 7: e34826, 2012.

Andersen RA, Essick GK, and Siegel RM. Neurons of area 7 activated by both visual stimuli and oculomotor behavior. *Exp Brain Res* 67: 316-322, 1987.

Anderson EJ, Mannan SK, Husain M, Rees G, Sumner P, Mort DJ, McRobbie D, and Kennard C. Involvement of prefrontal cortex in visual search. *Exp Brain Res* 180: 289-302, 2007.

Anderson JC, Kennedy H, and Martin KAC. Pathways of attention: synaptic relationships of frontal eye field to V4, lateral intraparietal cortex, and Area 46 in macaque monkey. *J Neurosci* 31: 10872, 2011.

Bichot NP, Rao SC, and Schall JD. Continuous processing in macaque frontal cortex during visual search. *Neuropsychologia* 39: 972-982, 2001a.

Bichot NP, and Schall JD. Effects of similarity and history on neural mechanisms of visual selection. *Nat Neurosci* 2: 549-554, 1999.

Bichot NP, and Schall JD. Priming in macaque frontal cortex during popout visual search: feature-based facilitation and location-based inhibition of return. *J Neurosci* 22: 4675, 2002.

Bichot NP, Schall JD, and Thompson KG. Visual feature selectivity in frontal eye fields induced by experience in mature macaques. 1996.

Bichot NP, Thompson KG, Rao SC, and Schall JD. Reliability of macaque frontal eye field neurons signaling saccade targets during visual search. *J Neurosci* 21: 713-725, 2001b.

Boehler CN, Tsotsos JK, Schoenfeld MA, Heinze HJ, and Hopf JM. Neural Mechanisms of Surround Attenuation and Distractor Competition in Visual Search. *J Neurosci* 31: 5213-5224, 2011.

Britten KH, Shadlen MN, Newsome WT, and Movshon JA. The analysis of visual motion: a comparison of neuronal and psychophysical performance. *J Neurosci* 12: 4745-4765, 1992.

Bruce CJ, and Goldberg ME. Primate frontal eye fields. I. Single neurons discharging before saccades. *J Neurophysiol* 53: 603-635, 1985.

Bruce CJ, Goldberg ME, Bushnell MC, and Stanton GB. Primate frontal eye fields. II. Physiological and anatomical correlates of electrically evoked eye movements. *J Neurophysiol* 54: 714, 1985.

Bundesen C, Habekost T, and Kyllingsbæk S. A neural theory of visual attention: Bridging cognition and neurophysiology. *Psychol Rev* 112: 291-328, 2005.

Burrows BE, and Moore T. Influence and limitations of popout in the selection of salient visual stimuli by area V4 neurons. *J Neurosci* 29: 15169, 2009.

Buschman TJ, and Miller EK. Top-down versus bottom-up control of attention in the prefrontal and posterior parietal cortices. *Science* 315: 1860, 2007.

Cohen JY, Heitz RP, Schall JD, and Woodman GF. On the origin of event-related potentials indexing covert attentional selection during visual search. *J Neurophysiol* 102: 2375, 2009a.

877 **Cohen JY, Heitz RP, Woodman GF, and Schall JD**. Neural basis of the set-
878 size effect in frontal eye field: timing of attention during visual search. *J*
879 *Neurophysiol* 101: 1699-1704, 2009b.
880 **Corbetta M**. Frontoparietal cortical networks for directing attention and the eye to
881 visual locations: Identical, independent, or overlapping neural systems? *P*
882 *Natl Acad Sci* 95: 831, 1998.
883 **Desimone R, and Duncan J**. Neural mechanisms of selective visual attention.
884 *Annu Rev Neurosci* 18: 193-222, 1995.
885 **Ding L, and Hikosaka O**. Comparison of reward modulation in the frontal eye
886 field and caudate of the macaque. *J Neurosci* 26: 6695, 2006.
887 **Duncan J, and Humphreys GW**. Visual search and stimulus similarity. *Psychol*
888 *Rev* 96: 433, 1989.
889 **Eimer M**. The N2pc component as an indicator of attentional selectivity.
890 *Electroencephalography and clinical neurophysiology* 99: 225-234, 1996.
891 **Eimer M, and Kiss M**. The top-down control of visual selection and how it is
892 linked to the N2pc component. *Acta Psychol* 135: 100, 2010.
893 **Eimer M, Kiss M, and Cheung T**. Priming of pop-out modulates attentional
894 target selection in visual search: Behavioural and electrophysiological
895 evidence. *Vision Res* 50: 1353-1361, 2010.
896 **Eimer M, Kiss M, Press C, and Sauter D**. The roles of feature-specific task set
897 and bottom-up salience in attentional capture: An ERP study. *Journal of*
898 *Experimental Psychology: Human Perception and Performance; Journal of*
899 *Experimental Psychology: Human Perception and Performance* 35: 1316,
900 2009.
901 **Ekstrom LB, Roelfsema PR, Arsenault JT, Bonmassar G, and Vanduffel W**.
902 Bottom-up dependent gating of frontal signals in early visual cortex. *Science*
903 321: 414, 2008.
904 **Givre SJ, Schroeder CE, and Arezzo JC**. Contribution of extrastriate area V4 to
905 the surface-recorded flash VEP in the awake macaque. *Vision Res* 34: 415-
906 428, 1994.
907 **Godlove DC, Emeric EE, Segovis CM, Young MS, Schall JD, and Woodman**
908 **GF**. Event-Related Potentials Elicited by Errors during the Stop-Signal Task.
909 I. Macaque Monkeys. *J Neurosci* 31: 15640-15649, 2011a.
910 **Godlove DC, Garr AK, Woodman GF, and Schall JD**. Measurement of the
911 extraocular spike potential during saccade countermanding. *J Neurophysiol*
912 106: 104, 2011b.
913 **Gregoriou GG, Gotts SJ, and Desimone R**. Cell-Type-Specific Synchronization
914 of Neural Activity in FEF with V4 during Attention. *Neuron* 73: 581-594, 2012.
915 **Heitz RP, Cohen JY, Woodman GF, and Schall JD**. Neural correlates of
916 correct and errant attentional selection revealed through N2pc and frontal
917 eye field activity. *J Neurophysiol* 104: 2433-2441, 2010.
918 **Helmholtz H**. Ueber einige Gesetze der Vertheilung elektrischer Ströme in
919 körperlichen Leitern mit Anwendung auf die thierisch-elektrischen Versuche.
920 *Annalen der Physik* 165: 211-233, 1853.

Hikosaka O, and Wurtz RH. Visual and oculomotor functions of monkey substantia nigra pars reticulata. IV. Relation of substantia nigra to superior colliculus. *J Neurophysiol* 49: 1285-1301, 1983.

Hopf JM, Boelmans K, Schoenfeld AM, Heinze HJ, and Luck SJ. How does attention attenuate target-distractor interference in vision?:: Evidence from magnetoencephalographic recordings. *Cognitive Brain Research* 15: 17-29, 2002.

Hopf JM, Boelmans K, Schoenfeld MA, Luck SJ, and Heinze HJ. Attention to features precedes attention to locations in visual search: Evidence from electromagnetic brain responses in humans. *J Neurosci* 24: 1822-1832, 2004.

Hopf JM, Luck SJ, Girelli M, Hagner T, Mangun GR, Scheich H, and Heinze HJ. Neural sources of focused attention in visual search. *Cereb Cortex* 10: 1233, 2000.

Itti L, and Koch C. Computational modelling of visual attention. *Nat Rev Neurosci* 2: 194-203, 2001.

Joseph JS, Chun MM, and Nakayama K. Attentional requirements in a'preattentive'feature search task. *Nature* 387: 805-807, 1997.

Katsuki F, and Constantinidis C. Early involvement of prefrontal cortex in visual bottom-up attention. *Nat Neurosci* 15: 1160-1166, 2012.

Katzner S, Nauhaus I, Benucci A, Bonin V, Ringach DL, and Carandini M. Local origin of field potentials in visual cortex. *Neuron* 61: 35-41, 2009.

Kiss M, Driver J, and Eimer M. Reward priority of visual target singletons modulates event-related potential signatures of attentional selection. *Psychol Sci* 20: 245-251, 2009.

Leonards U, Sunaert S, Van Hecke P, and Orban GA. Attention mechanisms in visual search-an fMRI study. *J Cognitive Neurosci* 12: 61-75, 2000.

Luck SJ. *An introduction to the event-related potential technique*. Cambridge: MIT Press, 2005.

Luck SJ, Chelazzi L, Hillyard SA, and Desimone R. Neural mechanisms of spatial selective attention in areas V1, V2, and V4 of macaque visual cortex. *J Neurophysiol* 77: 24, 1997a.

Luck SJ, Girelli M, McDermott MT, and Ford MA. Bridging the gap between monkey neurophysiology and human perception: An ambiguity resolution theory of visual selective attention. *Cognitive Psychol* 33: 64-87, 1997b.

Luck SJ, and Hillyard SA. Electrophysiological correlates of feature analysis during visual search. *Psychophysiology* 31: 291-308, 1994a.

Luck SJ, and Hillyard SA. Electrophysiological evidence for parallel and serial processing during visual search. *Atten Percept Psycho* 48: 603-617, 1990.

Luck SJ, and Hillyard SA. Spatial filtering during visual search: Evidence from human electrophysiology. *J Exp Psychol Human* 20: 1000, 1994b.

Maljkovic V, and Nakayama K. Priming of pop-out: I. Role of features. *Mem Cognition* 22: 657-672, 1994.

Mitzdorf U. Current source-density method and application in cat cerebral cortex: investigation of evoked potentials and EEG phenomena. *Physiol Rev* 65: 37, 1985.

Monosov IE, Sheinberg DL, and Thompson KG. The Effects of Prefrontal Cortex Inactivation on Object Responses of Single Neurons in the Inferotemporal Cortex during Visual Search. *J Neurosci* 31: 15956-15961, 2011.

Monosov IE, Sheinberg DL, and Thompson KG. Paired neuron recordings in the prefrontal and inferotemporal cortices reveal that spatial selection precedes object identification during visual search. *P Natl Acad Sci* 107: 13105-13110, 2010.

Monosov IE, and Thompson KG. Frontal eye field activity enhances object identification during covert visual search. *J Neurophysiol* 102: 3656-3672, 2009.

Monosov IE, Trageser JC, and Thompson KG. Measurements of simultaneously recorded spiking activity and local field potentials suggest that spatial selection emerges in the frontal eye field. *Neuron* 57: 614-625, 2008.

Moore T, and Armstrong KM. Selective gating of visual signals by microstimulation of frontal cortex. *Nature* 421: 370-373, 2003.

Muggleton NG, Juan CH, Cowey A, and Walsh V. Human frontal eye fields and visual search. *J Neurophysiol* 89: 3340-3343, 2003.

Ninomiya T, Sawamura H, Inoue K, and Takada M. Segregated Pathways Carrying Frontally Derived Top-Down Signals to Visual Areas MT and V4 in Macaques. *J Neurosci* 32: 6851-6858, 2011.

Nunez PL, and Srinivasan R. *Electric fields of the brain: the neurophysics of EEG*. Oxford University Press, USA, 2006.

Orban GA, Van Essen D, and Vanduffel W. Comparative mapping of higher visual areas in monkeys and humans. *Trends Cogn Sci* 8: 315-324, 2004.

Pouget P, Emeric EE, Stuphorn V, Reis K, and Schall JD. Chronometry of visual responses in frontal eye field, supplementary eye field, and anterior cingulate cortex. *J Neurophysiol* 94: 2086, 2005.

Pouget P, Stepniewska I, Crowder EA, Leslie MW, Emeric EE, Nelson MJ, and Schall JD. Visual and motor connectivity and the distribution of calcium-binding proteins in macaque frontal eye field: implications for saccade target selection. *Front Neuroanat* 3: 1-14, 2009.

Purcell BA, Weigand PK, and Schall JD. Supplementary Eye Field during Visual Search: Salience, Cognitive Control, and Performance Monitoring. *J Neurosci* 32: 10273-10285, 2012.

Reinhart RM, Carlisle NB, Kang MS, and Woodman GF. Event-related potentials elicited by errors during the stop-signal task. II: Human effector specific error responses. *J Neurophysiol* 2012a.

Reinhart RM, Heitz RP, Purcell BA, Weigand PK, Schall JD, and Woodman GF. Homologous mechanisms of visuospatial working memory maintenance in macaque and human: Properties and sources. *J Neurosci* 2012b.

Sato T, Murthy A, Thompson KG, and Schall JD. Search efficiency but not response interference affects visual selection in frontal eye field. *Neuron* 30: 583-591, 2001.

Schmolesky MT, Wang Y, Hanes DP, Thompson KG, Leutgeb S, Schall JD, and Leventhal AG. Signal timing across the macaque visual system. *J Neurophysiol* 79: 3272, 1998.

Theeuwes J. Top-down and bottom-up control of visual selection: Reply to commentaries. *Acta Psychol* 135: 133-139, 2010.

Thomas NWD, and Pare M. Temporal processing of saccade targets in parietal cortex area LIP during visual search. *J Neurophysiol* 97: 942-947, 2007.

Thompson KG, and Bichot NP. A visual salience map in the primate frontal eye field. *Prog Brain Res* 147: 249-262, 2005.

Thompson KG, Bichot NP, and Schall JD. Dissociation of visual discrimination from saccade programming in macaque frontal eye field. *J Neurophysiol* 77: 1046-1050, 1997.

Thompson KG, Biscoe KL, and Sato TR. Neuronal basis of covert spatial attention in the frontal eye field. *J Neurosci* 25: 9479, 2005.

Thompson KG, Hanes DP, Bichot NP, and Schall JD. Perceptual and motor processing stages identified in the activity of macaque frontal eye field neurons during visual search. *J Neurophysiol* 76: 4040-4055, 1996.

Treisman A, and Gormican S. Feature analysis in early vision: Evidence from search asymmetries. *Psychol Rev* 95: 15-48, 1988.

Treisman A, and Sato S. Conjunction search revisited. *J Exp Psychol Human* 16: 459, 1990.

Treisman AM, and Gelade G. A feature-integration theory of attention. *Cognitive Psychol* 12: 97-136, 1980.

Wardak C, Ibos G, Duhamel JR, and Olivier E. Contribution of the monkey frontal eye field to covert visual attention. *J Neurosci* 26: 4228-4235, 2006.

Wardak C, Vanduffel W, and Orban GA. Searching for a salient target involves frontal regions. *Cereb Cortex* 20: 2464-2477, 2010.

Wolfe JM. Guided Search 4.0: Current Progress with a model of visual search. In: *Integrated models of cognitive systems*, edited by W. G. New York: Oxford, 2007, p. 99-119.

Wolfe JM. What can 1 million trials tell us about visual search? *Psychol Sci* 9: 33-39, 1998.

Woodman GF. Homologues of human ERP components in nonhuman primates. The Oxford Handbook of ERP Components. New York: Oxford University Press, 2011.

Woodman GF, Kang MS, Rossi AF, and Schall JD. Nonhuman primate event-related potentials indexing covert shifts of attention. *P Natl Acad Sci* 104: 15111, 2007.

Woodman GF, Kang MS, Thompson K, and Schall JD. The effect of visual search efficiency on response preparation. *Psychol Sci* 19: 128-136, 2008.

Woodman GF, and Luck SJ. Electrophysiological measurement of rapid shifts of attention during visual search. *Nature* 400: 867-869, 1999.

Woodman GF, and Luck SJ. Serial deployment of attention during visual search. *J Exp Psychol Human* 29: 121, 2003.

Young MH, Heitz R, Purcell B, Schall J, and Woodman G. Source localization of an event-related potential indexing covert shifts of attention in macaques. *J Vis* 11: 194-194, 2011.

Zeki SM. Cortical projections from two prestriate areas in the monkey. *Brain Res* 34: 19, 1971.

Zhou H, and Desimone R. Feature-based attention in the frontal eye field and area V4 during visual search. *Neuron* 70: 1205-1217, 2010.

FIGURE CAPTIONS

Figure 1. Visual search task and behavior. **A**, After fixating for a variable delay, a search array appeared consisting of one target (e.g., green disk) and 1, 3, or 7 distractors (e.g., red disks). Monkeys were required to make a single saccade to the target for reward. Target identity varied across sessions. **B**, We directly compared our new results from efficient pop-out search with previously published data collected from the same monkeys performing an inefficient visual search task (Cohen et al. 2009a). All procedures were identical to efficient search except that the monkeys searched for a T versus L (or vice versa). **C**, mean response time (RT) to the target as a function of set size for both search tasks. Error bars represent SE around the mean of the session means. Asterisks indicate significant differences in slope across tasks (*** for $p < 0.001$).

Figure 2. Target selection during a representative session. Average activity of one neuron (**A**), LFP site (**B**), and ERP over visual cortex (**C**) when the search target was inside (dark) and opposite (light) the receptive field (or preferred location) of the signal. Bands around average activity indicate 95% confidence intervals. Vertical lines indicate selection time when the two curves became significantly different. Bands around selection time indicate SE estimated using a bootstrap procedure (100 samples). Solid triangle indicates mean response time for this session.

Figure 3. Population selection times for each type of signal. Cumulative distributions of selection times measured from intracranial FEF single-unit spiking (blue), FEF LFPs (green), and the posterior m-N2pc (red) during pop-out search. Selection precedes saccadic response time (RT, dashed grey line).

Figure 4. Within-session selection time differences across signals. Differences between selection time measured from simultaneously recorded m-N2pc and FEF single-unit spikes (**A**), mN2pc and FEF LFPs (**B**), and FEF LFPs and single-unit spikes (**C**). The solid vertical line indicates the mean of the distribution. The dashed vertical line indicates zero. Asterisks indicate significant differences from zero (Wilcoxon rank-sum test, *** for $p < 0.001$; n.s. for nonsignificant).

Figure 5. Average selection time for FEF single-unit spikes (top), FEF LFPs (middle), and m-N2pc (bottom) at each set size. Asterisks indicate significant difference in slope across efficient (pop-out) and inefficient (T versus L) search (multiple linear regression; * for $p < 0.05$; ** for $p < 0.01$; *** for $p < 0.001$). Error bars indicate SE.

Figure 6. Average magnitude of selection (response amplitude when the target was in the preferred location of the signal minus the response amplitude when a distractr was in the preferred location) for FEF single-unit spikes, FEF LFPs, and the m-N2pc at each set size. Conventions as in Figure 5.

Figure 7. Trial-by-trial correlations between FEF LFP amplitude and the amplitude difference between posterior EEG electrodes (**A**), between FEF LFP amplitude and FEF single-unit firing rate recorded on the same electrode (**B**), and between FEF single-unit firing rate and the amplitude difference between posterior EEG electrodes (**C**). Asterisks indicate significance from zero, indicated by the vertical dashed line (Wilcoxon rank-sum; n.s. for nonsignificance; ** for $p < 0.01$; *** for $p < 0.001$).

Figure 8. Selection time by number of trials. A: average selection time as a function of number of trials (randomly sampled, with replacement) across recordings of FEF single-units (blue), LFP (green), and m-N2pc (red). The black point (with SE line) indicates the average number of trials in our data set. B: decay parameter (τ) estimates from exponential fits to the selection time by number of trials. C: asymptote parameter (TST_{min}) estimates from the exponential fits plotted in B.

Table 1. Response time and selection time search slopes, in ms/items, for each neural signal during efficient (pop-out) and inefficient visual search. Values are slope of linear regression ± SE. Asterisks indicate significant slope coefficient for set size: *p < 0.05; **p < 0.01; ***p < 0.001. Pairwise comparisons indicate significant interaction term for set size and task. Inefficient search data have been previously described (Cohen et al., 2009a).

Table 2. Comparisons of selection time and latency of visual onset across signals during efficient (pop-out) search. Values are means ± SE. Brackets with asterisks indicate significant differences between signals (Wilcoxon rank-sum test). Asterisks alone indicate significant difference from zero (Wilcoxon signed-rank test). * for $P < 0.05$; ** for $P < 0.001$.

Table 1. *Response time and selection time search slopes, in ms/items, for each neural signal during efficient (pop-out) and inefficient visual search.*

	Monkey Q		Monkey S	
Response time				
Inefficient	22.6 ± 1.6 ***	***	10.5 ± 1.4 ***	***
Efficient	2.3 ± 0.8 *		0.7 ± 1.0	
FEF single-units				
Inefficient	4.6 ± 1.5 ***	***	5.3 ± 1.7 ***	
Efficient	1.2 ± 1.1		2.3 ± 1.1	
FEF LFP				
Inefficient	8.2 ± 1.4 ***	***	6.3 ± 1.3 ***	***
Efficient	1.1 ± 1.0		0.4 ± 1.5	
m-N2pc				
Inefficient	9.7 ± 0.5 ***	***	6.2 ± 0.9 ***	
Efficient	0.9 ± 1.0		1.0 ± 0.9	

Values are slope of linear regression ± SE. Asterisks indicate significant slope coefficient for set size: *p < 0.05; **p < 0.01; ***p < 0.001. Pairwise comparisons indicate significant interaction term for set size and task. Inefficient search data have been previously described (Cohen et al., 2009a).

Table 2. *Comparisons of target selection time and latency of visual onset across signals during efficient (pop-out) search.*

	Monkey Q		Monkey S	
Visual onset time, ms				
Single-units	71 ± 3.8	**	66 ± 2.6	*
LFP	52 ± 1.9	**	61 ± 2.6	*
ERP	67 ± 3.1		68 ± 4.6	
Selection time, ms				
Single-units	155 ± 4.2		160 ± 5.6	
LFP	160 ± 3.7	*	167 ± 6.1	**
ERP	168 ± 4.1		203 ± 4.2	**
Selection time difference				
ERP - Single-units	9 ± 4.3		39 ± 4.6	**
ERP - LFP	6 ± 2.6	*	31 ± 4.7	**
LFP - Single-units	3 ± 3.2		8 ± 4.6	

Values are means ± SE. Brackets with asterisks indicate significant differences between signals (Wilcoxon rank-sum test). Asterisks alone indicate significant difference from zero (Wilcoxon signed-rank test). * for $P < 0.05$; ** for $P < 0.001$

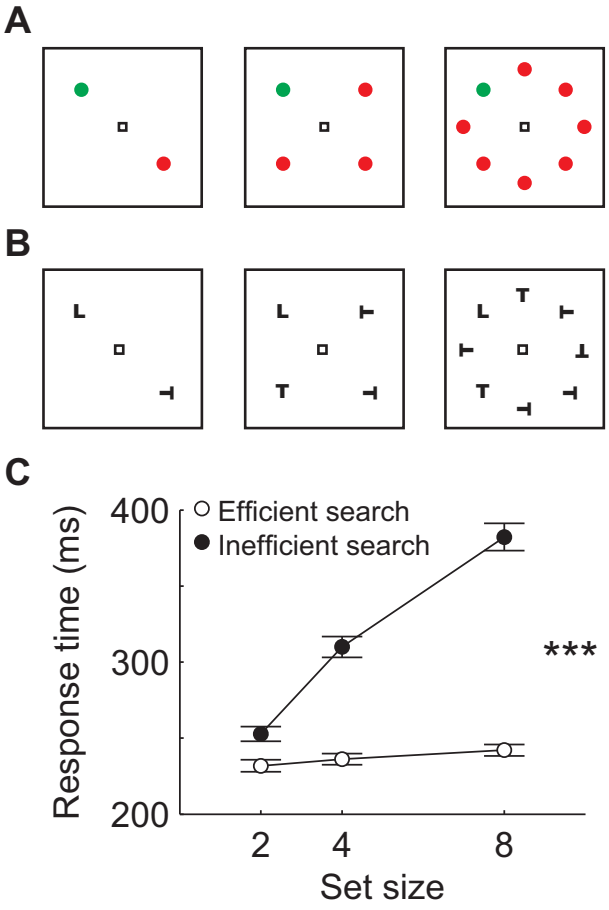
A
B
C
400
300
200
Response time (ms)
Efficient search
Inefficient search
***
2
4
8
Set size

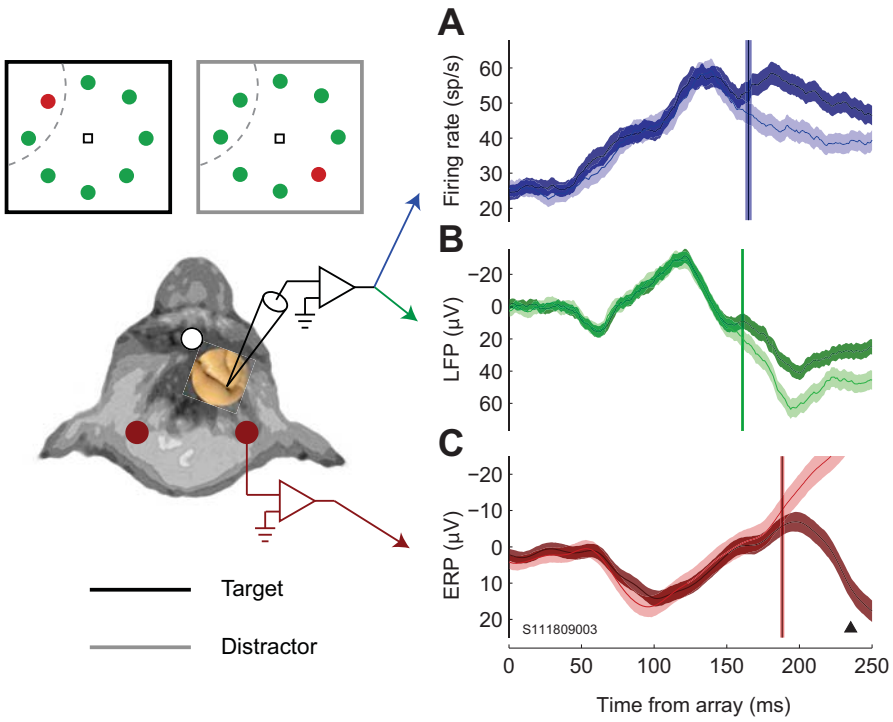
A
Firing rate (sp/s)
60
50
40
30
20
B
LFP (μV)
−20
0
20
40
60
C
ERP (μV)
−20
−10
0
10
20
S111809003
0
50
100
150
200
250
Time from array (ms)
Target
Distractor

Figure 3

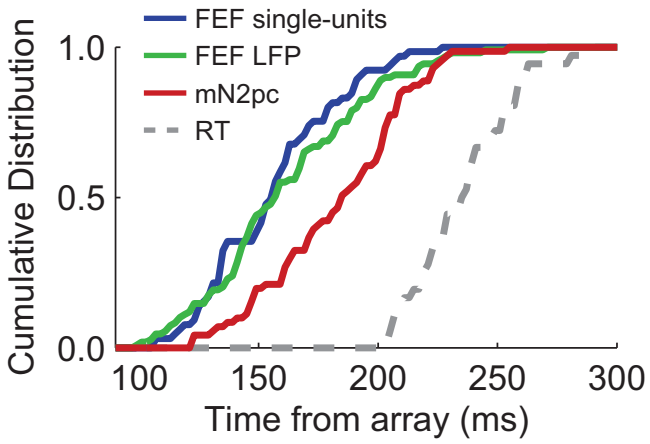
FEF single-units
FEF LFP
mN2pc
RT
Cumulative Distribution
1.0
0.5
0.0
100
150
200
250
300
Time from array (ms)

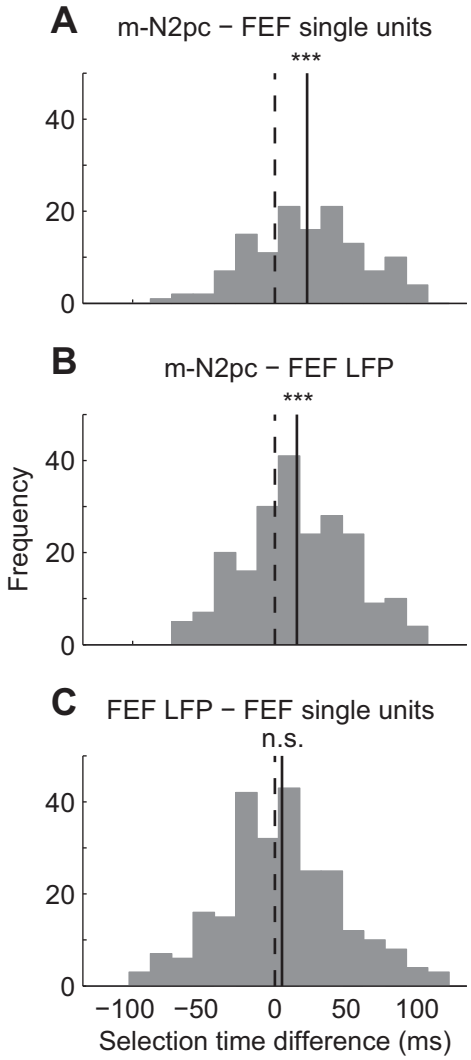
A
m-N2pc − FEF single units
***
40
20
0
B
m-N2pc − FEF LFP
***
Frequency
40
20
0
C
FEF LFP − FEF single units
n.s.
40
20
0
−100
−50
0
50
100
Selection time difference (ms)

Figure 5

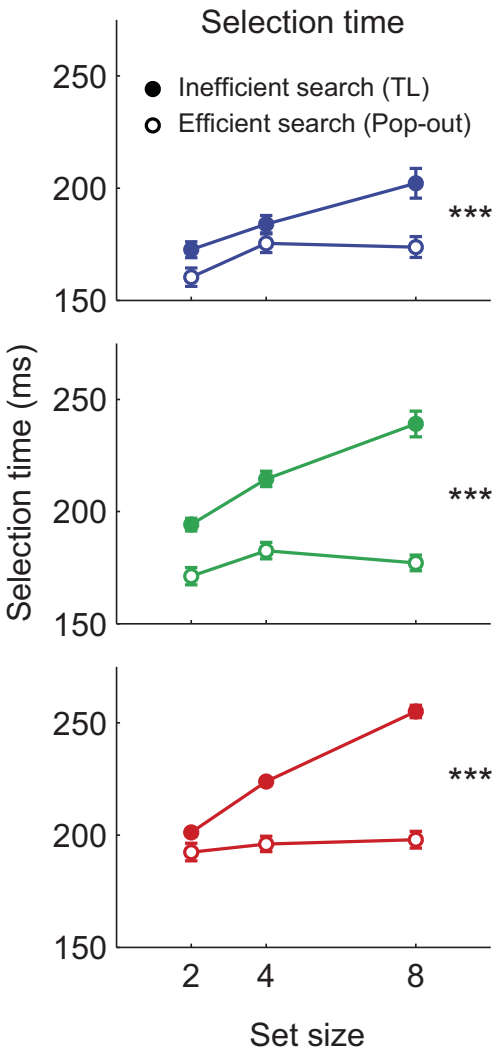
Selection time
Inefficient search (TL)
Efficient search (Pop-out)
Selection time (ms)
250
200
150
***
***
***
2
4
8
Set size

Figure 6

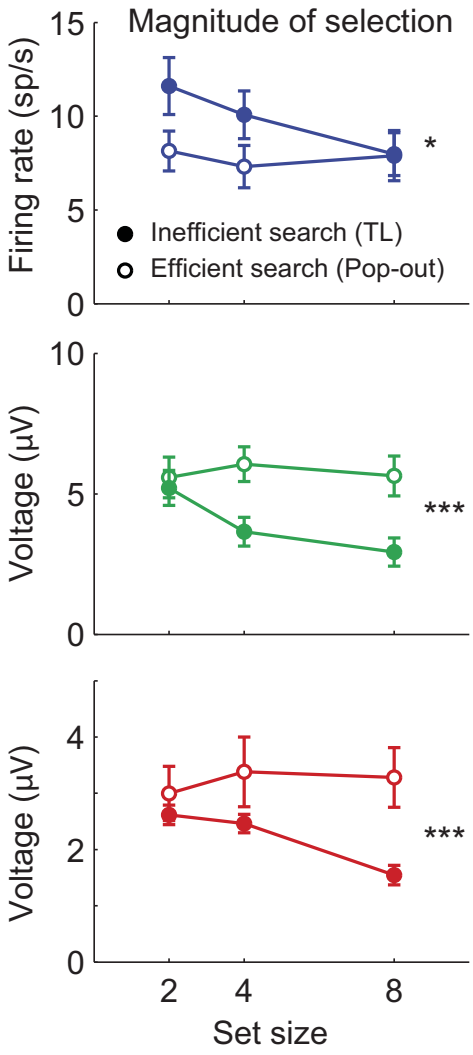
Magnitude of selection
Firing rate (sp/s)
15
10
5
0
Inefficient search (TL)
Efficient search (Pop-out)
*
Voltage (μV)
10
5
0
***
Voltage (μV)
4
2
0
***
2
4
8
Set size

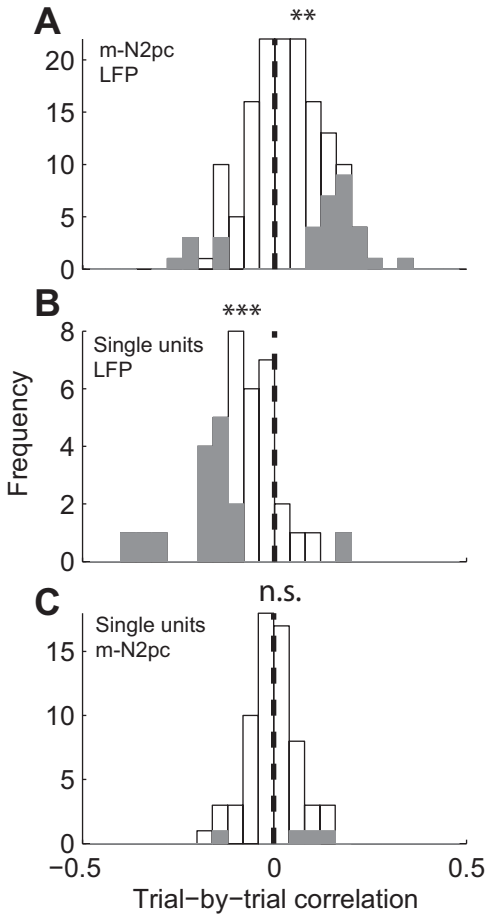
A
**
m-N2pc
LFP
20
15
10
5
0
B
***
Single units
LFP
8
6
4
2
0
Frequency
C
n.s.
Single units
m-N2pc
15
10
5
0
−0.5
0
0.5
Trial−by−trial correlation

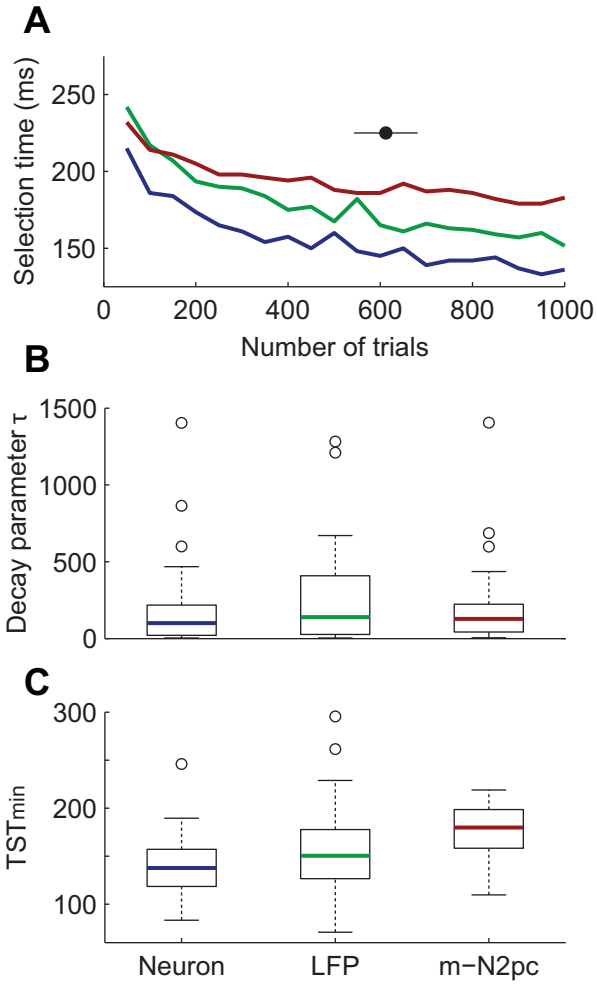
A
Selection time (ms)
250
200
150
0
200
400
600
800
1000
Number of trials
B
Decay parameter τ
1500
1000
500
0
C
TSTmin
300
200
100
Neuron
LFP
m−N2pc